Electronic Supplementary Material (ESI) for Nanoscale Horizons.

Supplementary material

Elucidating the special role of strong metal-support interactions in Pt/MnO_2 catalysts for total toluene oxidation

Shengpeng Mo,[a] Qi Zhang,[a] Mingyuan Zhang,[a] Qian Zhang,[a] Jiaqi Li,[a] Mingli Fu,[a, b, c] Junliang Wu,[a, b, c] Peirong Chen[a, b, c] and Daiqi Ye[a,b,c] *

[a] *School of Environment and Energy, South China University of Technology, Guangzhou 510006, China*

[b] *Guangdong Provincial Key Laboratory of Atmospheric Environment and Pollution Control (SCUT), Guangzhou 510006, China*

[c] *Guangdong Provincial Engineering and Technology Research Centre for Environmental Risk Prevention and Emergency Disposal, South China University of Technology, Guangzhou Higher Education Mega Centre, Guangzhou 510006, China*

* *Corresponding author at: School of Environment and Energy, South China University of Technology, Guangzhou 510006, China*
E-mail address: cedqye@scut.edu.cn (D. Ye);

Experimental section

Synthesis of Pt nanoparticles

Pt nanoparticles (NPs) were synthesized by a glycol reduction method. In detail, 2.5 mL chloroplatinic acid (20 g/L H_2PtCl_6 solution) and 220 mg polyvinylpyrrolidone (PVP, k29-32, Mw=58000) were dissolved in a 100 mL round-bottom flask with a 25 mL glycol to obtain a yellow solution. After stirring, the yellow solution was heated to about 120 °C for 1 h under magnetic stirring, until the yellow solution changed to a dark-brown solution. Finally, 60 mL acetone was slowly added to dark-brown solution to extract Pt NPs after cooled down to room temperature, and the Pt NPs were collected by centrifugation (6000 rpm, 5 min). The as-obtained nanoparticles were washed with n-hexane several times, and then dispersed into ethanol.

Synthesis of carbon spheres

The as-obtained carbon spheres are used as templates to prepare later hollow γ-MnO_2 structure. In a typical procedure, glucose (5.6 g) was dissolved in a 50 mL deionized water. After stirred for 30 min, the reaction solution was transferred into a 100 mL stainless steel autoclave at 180 ^oC for 24 h. After cooled to room temperature, the as-obtained precipitates were washed with deionized water and ethanol several times. Finally, the brown precipitates were dried at 100 ^oC for 12 h.

Synthesis of different MnO_2 crystal structures

α-MnO_2 structure. $KMnO_4$ (100 mmol) and $MnSO_4$ (150 mmol) were dissolved into 400 mL and 100 mL deionized water, respectively. Then, the $KMnO_4$ solution was added in the $MnSO_4$ solution. After that, 12 mL concentrated nitric acid (68%) was introduced into the former solution with strongly stirring. The dark brown slurry was formed after refluxed at 100 ^oC for 24 h, and then cooled to room temperature. The as-obtained precipitates were washed with deionized water and ethanol several times. Finally, the brown precipitates were dried at 100 ^{o}C for 12 h.

β-MnO$_2$ structure. $(NH_4)_2S_2O_8$ (10 mmol) and an equal amount of $MnSO_4$ (10mmol) were added into 85 mL deionized water to get a homogeneous solution, which was put into a 100 mL stainless steel autoclave, sealed and kept at 120 ^{o}C for 12 h, then cooled to room temperature. The as-obtained black precipitates were washed with deionized water and ethanol several times, and dried at 100 ^{o}C for 12 h.

γ-MnO$_2$ structure. NH_4HCO_3 (48 mmol) and 50 wt.% $Mn(NO_3)_2$ (20 mmol) were added into 100 mL and 100 mL deionized water, respectively. The NH_4HCO_3 solution was added in the $Mn(NO_3)_2$ solution under vigorous stirring, and the mixed solution was aged for 4 h at room temperature. The final white precipitates were filtered and washed several times with water and ethanol, then dried at 100 ^{o}C for 12 h. The white precipitates were heated at 400 ^{o}C for 4 h (a heating rate 2 ^{o}C min^{-1}) in air.

H-MnO$_2$ structure. 0.5 g carbon spheres as templates were dispersed into 100 mL $Mn(NO_3)_2$ (20 mmol) aqueous solution. The subsequent steps on the synthesis of the hollow MnO_2 catalysts were the same as γ-MnO$_2$ structure, in which the carbon spheres were decomposed at high temperature.

Synthesis of Pt-supported catalysts

Pt-supported catalysts were synthesized by an electrostatic chemical adsorption method. Typically, 1.0 g different MnO_2 supports were dispersed into 30 mL ethanol. Then a certain of pre-synthetic Pt NPs (loading content of about 0.4 wt%) dispersed into ethanol was added to the former solution. After stirring for 4 h, the powders were collected and washed twice times, and dried in oven at 100 °C for 12 h. The black powders were heated at 300 °C for 4 h (a heating rate 2 °C min^{-1}) in air.

Material characterizations

X-ray powder diffraction (XRD) patterns of the monolithic samples were performed by using a Panalytical X'Pert PRO system with Cu-Kα (λ=1.5406Å) radiation operated at 40kV and 40mA. The data were collected with at a scan rate of 10° min^{-1} within the range of scattering angle 2θ of 5 to 90°.

The Pt-based catalysts were determined by an inductively coupled plasma optical emission spectrometer (ICP-OES, iCAP 6300).

The size and morphology of samples were characterized by using field-emission scanning electron microscopy (FESEM, JEOL JSM-6700F) with an acceleration voltage of 15 kV, 10 mM. The microstructures of the samples were characterized on a transmission electron microscope (TEM, JEOL JEM-2010F) at a voltage of 200 kV.

A Micromeritics ASAP2020 was used to measure the surface areas and pore size distribution of the samples at −196 °C. Before the tests, the corresponding samples were degassed at 150 °C for 6 h to remove physically adsorbed impurities.

The hydrogen temperature programmed reduction (H_2-TPR) and oxygen temperature programmed desorption (O_2-TPD) measurement was measured on an Automated Catalyst Characterization System (Autochem 2920, MICROMERITICS) equipped with a thermal conductivity detector (TCD). The corresponding samples (50 mg) placed in a quartz reactor was pre-heated in 5% O_2/He flow from room temperature to 300 °C and held for 1 h (30 mL min^{-1}), and then cooling to room temperature. The catalysts were heated from room temperature to 800 °C with a constant rate of 10 °C min^{-1} under a gas flow (5% H_2/Ar, 30 mL min^{-1}).

The temperature programmed desorption of O_2 (O_2-TPD) with 0.1 g catalysts was pre-heated in 5% O_2/He flow from room temperature to 300 °C and held for 1 h (30 mL min^{-1}), and then cooling to room temperature. The catalysts were heated from room temperature to 800 °C at 10 °C min^{-1} in pure He (30 mL min^{-1}).

The thermal gravimetric analysis (TGA) of samples was performed using an HCT-2

TGA/DTA system in air with a heating-rate of 10 °C min^{-1} up to 700 °C under different atmospheres (N_2 or Air).

X–ray photoelectron spectroscopy (XPS) measurement was performed by using an XLESCALAB 250Xi electron spectrometer from VG Scientific with monochromatic Al Ka (1486.6 eV) radiation, and the binding energy was calibrated based on the C 1s peaks at 284.8 eV.

The reaction mechanism assessment of toluene oxidation was performed by in-situ diffuse reflectance infrared Fourier transform spectroscopy (DRIFTS, Thermo Fisher, America). Before recording of toluene oxidation, the monolithic catalyst was pre-treated by N_2 for 1h at 300 °C, then cooled to room temperature.

Quasi in-situ X–ray photoelectron spectroscopy (XPS) measurement was performed at an XLESCALAB 250Xi electron spectrometer from VG Scientific with monochromatic Al Ka (1486.6 eV) radiation, Germany. The setup consisted of a reaction cell attached to a set of differentially pumped electrostatic lenses and a separately pumped analyzer. Typically, the powder sample was pressed into a tantalum grid (to minimize potential charging effects), fixed to a sample holder and mounted inside the XPS reaction cell in front of the first aperture of the differentially pumped electrostatic lens system. The heating of the samples was done from the back using an infrared laser. The sample was pretreated in the XPS reaction cell by air at 300 °C until all residual surface carbon and carbonates disappeared. After cooling the sample to RT, the sample was heated to 150 °C and 250 °C with a heating rate of 5 °C min^{-1}, the atmosphere was changed to N_2 or Air. After cooling the sample to RT, the photoemission spectra were recorded.

Catalytic activity measurements

The catalytic activity was carried out in a fixed-bed quartz tubular micro-reactor (Φ = 10.0 mm) with 100 mg catalyst and 400 mg quartz sands (40–60 mesh). The volumetric composition of the reactant mixture was 1000 ppm toluene containing synthetic air (20% O_2 + balance N_2), and the total continuous flow was 100 mL min^{-1}, corresponding to a weight hourly space velocity (WHSV) of 60,000 mL g^{-1} h^{-1}. The range of temperature was 100 to 280 °C. The concentrations of the reactants and products were monitored online by gas chromatography (Shimadzu GC-2014) equipped with two flame ionization detector (FID). To study the effect of water vapor on the catalytic activity, the on-stream toluene oxidation experiment was carried out in the presence and absence of different water vapor (1.0 vol.%, 2.0 vol.%, 5.0 vol.% and 10 vol.%) obtained by bubbling. The toluene conversions (η_{toluene}, %) were calculated according to the following equation:

$$\eta_{\text{toluene}} = \frac{C_{\text{toluene,in}} - C_{\text{toluene,out}}}{C_{\text{toluene,in}}} \times 100\% \tag{1}$$

Where η_{toluene}, $C_{\text{toluene, in}}$ (ppm) and $C_{\text{toluene, out}}$ (ppm) are the toluene conversion, toluene in the inlet and outlet gas, respectively.

Catalytic activity can also be evaluated by comparing the apparent activation energy (E_a) values of catalysts, a sample with a lower E_a value in a catalytic reaction will possess excellent catalytic activity. It has been reported that VOCs combustion follows first-order kinetics at VOCs concentration less than 20% under presence of excess oxygen with the equations:

$$\gamma_{\text{toluene}} = \frac{N_{\text{toluene}} \times \eta_{\text{toluene}}}{W_{cat}} \tag{2}$$

$$\gamma_{toluene} = -\kappa c = \left[-A \exp\left(-\frac{E_a}{RT} \right) \right] c \tag{3}$$

Where N_{toluene}, W_{cat}, γ, κ, A, and E_a correspond to the C_{toluene} gas flow rate (mol s^{-1}), catalyst weight (g), reaction rate (μmol g^{-1} s^{-1})), rate constant (s^{-1}), pre-exponential factor, and apparent activation energy (kJ mol^{-1}), respectively. The κ values are calculated from the reaction rates and toluene conversions.

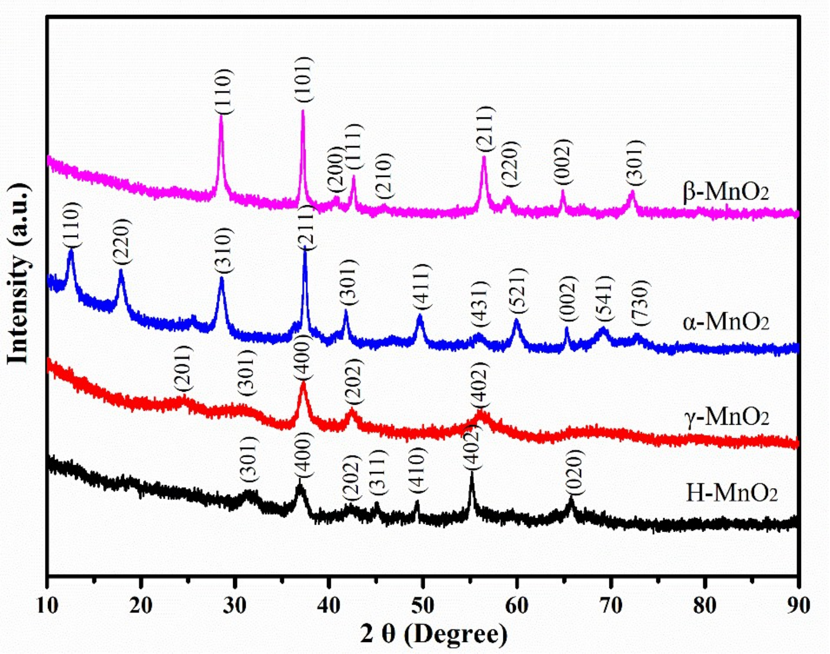

Fig. S1 XRD patterns of different MnO_2 samples.

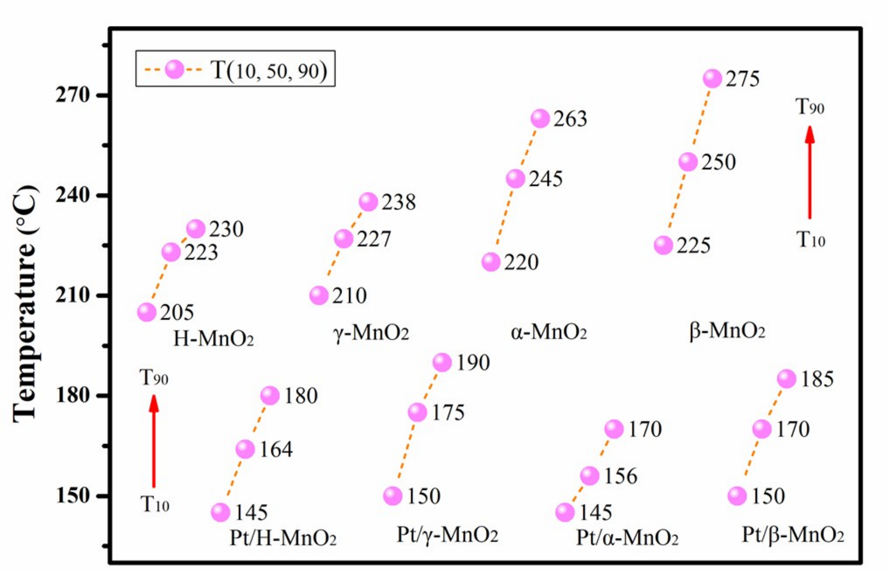

Fig. S2 T_{10}, T_{50} and T_{90} for the toluene oxidation over different MnO_2 and Pt/MnO_2 samples. Toluene concentration was 1000 ppm balanced air, and all the reactions were kept at WHSV=60, 000 mL g^{-1} h^{-1}.

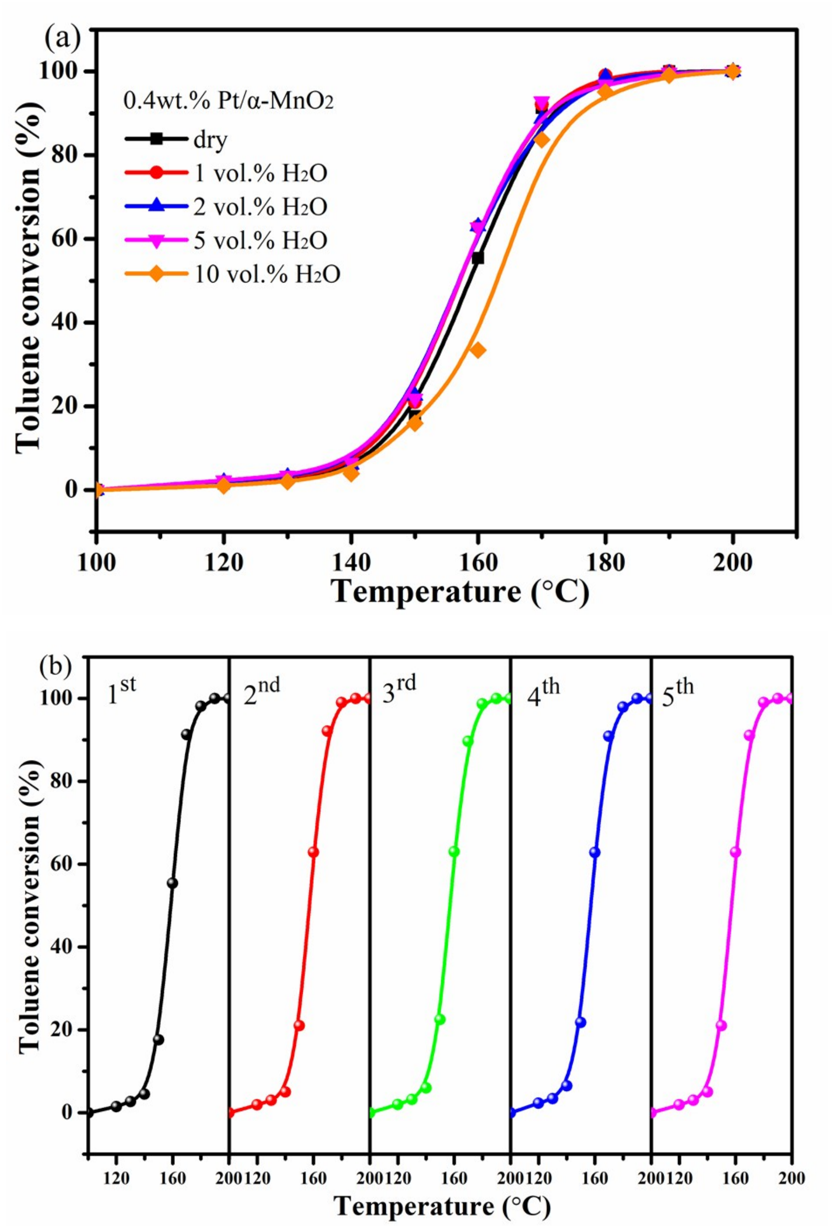

Fig. S3 (a) The effect of water vapor on toluene conversion over the Pt/α-MnO_2 catalyst under different amounts of water vapor, and (b) cycling test of Pt/α-MnO_2 catalyst at different temperatures. Toluene concentration was 1000 ppm balanced air, and all the reactions were kept at WHSV=60, 000 mL g^{-1} h^{-1}.

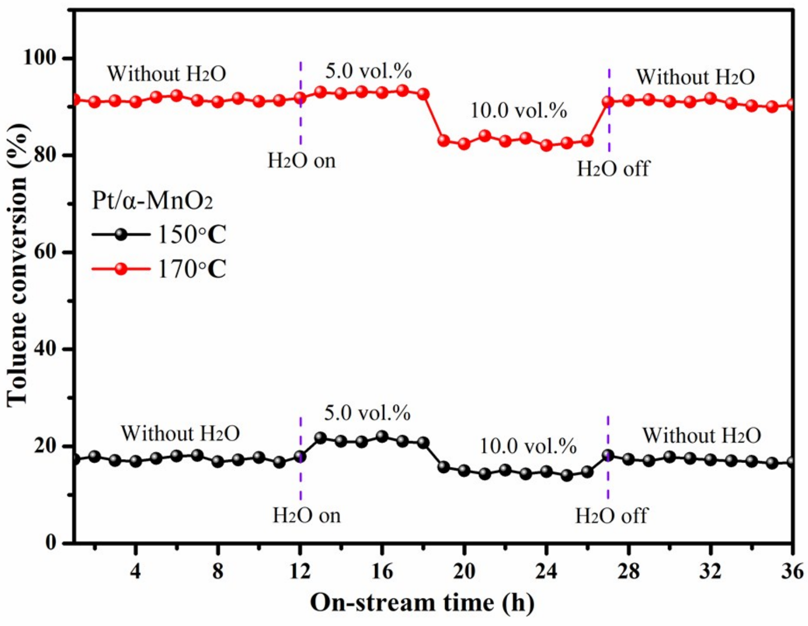

Fig. S4 the Catalytic activity versus on-stream time over Pt/α-MnO_2 catalyst at 150 and 170 °C. Toluene concentration was 1000 ppm balanced air, and all the reactions were kept at WHSV=60, 000 mL g^{-1} h^{-1}.

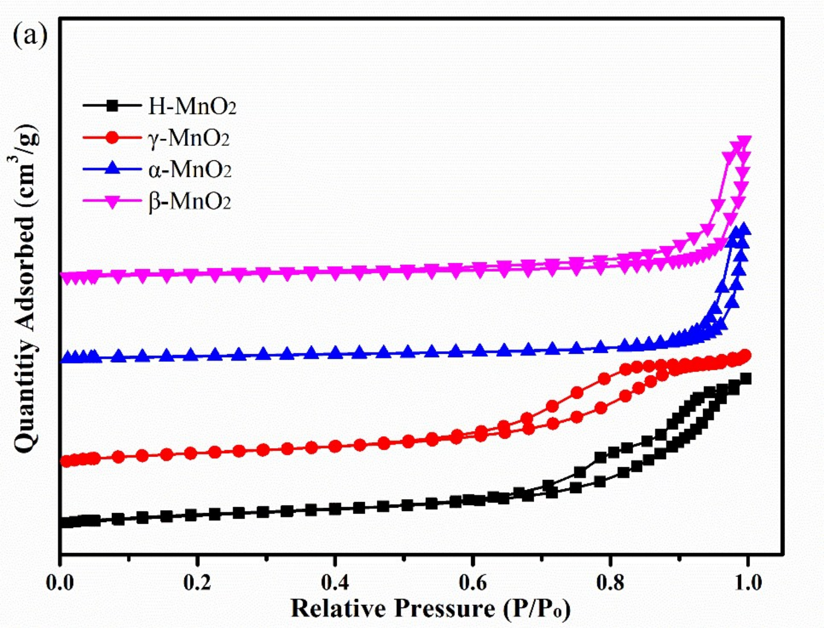
(a)
H-MnO2
γ-MnO2
α-MnO2
β-MnO2
Quantitiy Adsorbed (cm3/g)
0.0
0.2
0.4
0.6
0.8
1.0
Relative Pressure (P/Po)

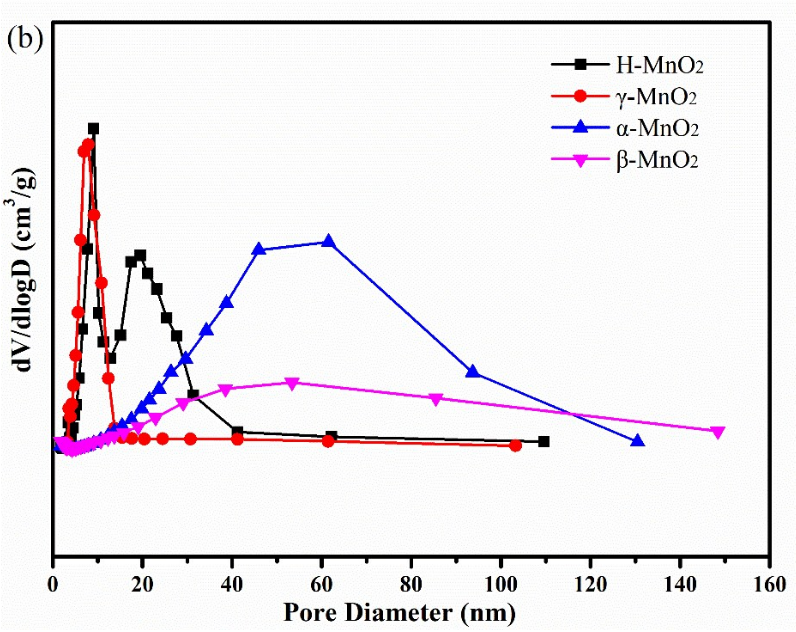
(b)
H-MnO2
γ-MnO2
α-MnO2
β-MnO2
dV/dlogD (cm3/g)
0
20
40
60
80
100
120
140
160
Pore Diameter (nm)

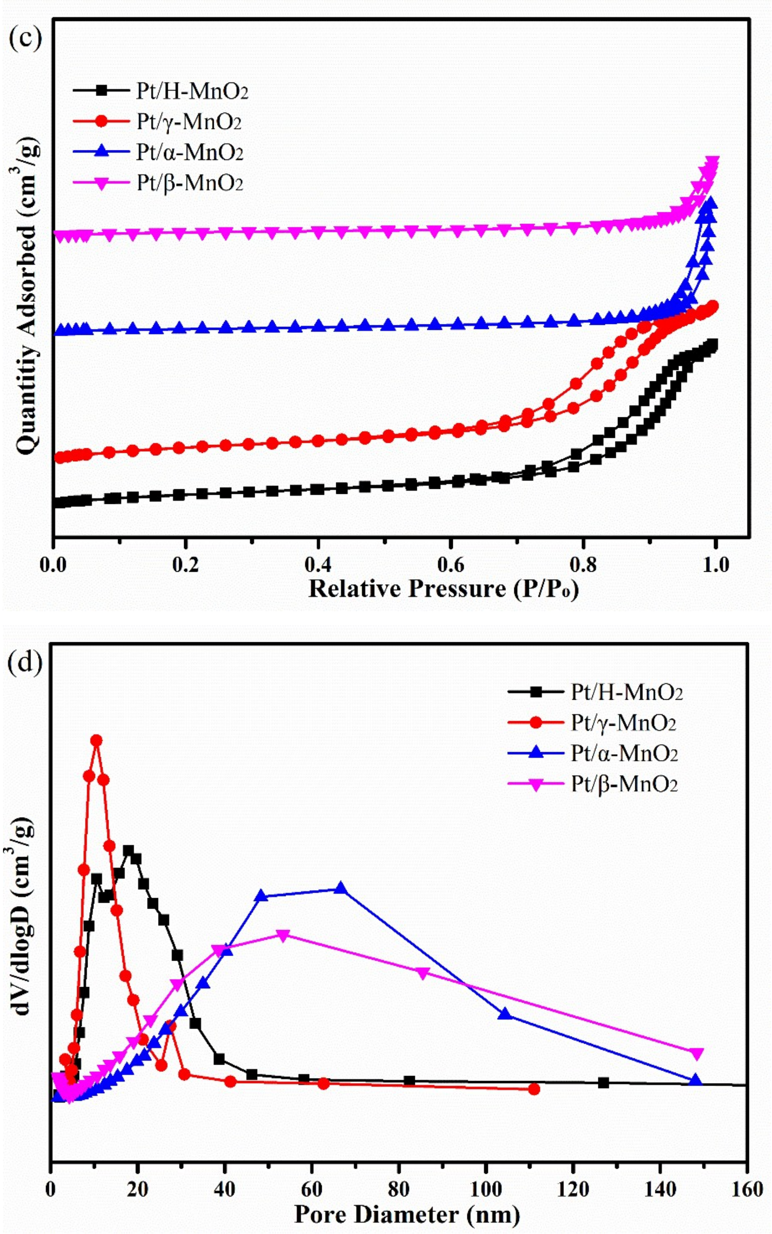

Fig. S5 (a, c) N_2 adsorption−desorption isotherms and (b, d) pore size distributions of different MnO_2 and Pt/MnO_2 samples.

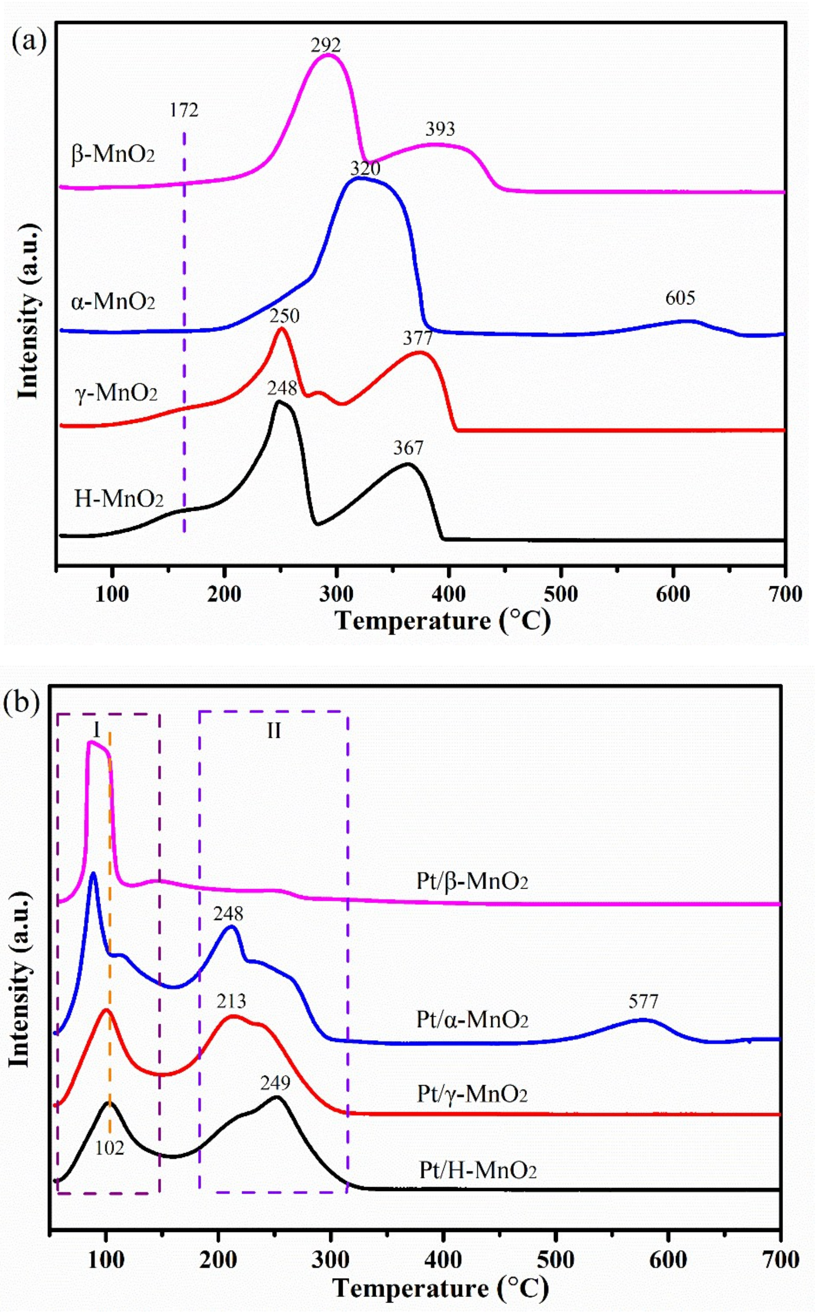

Fig. S6 H_2-TPR profiles of different MnO_2 and Pt/MnO_2 samples.

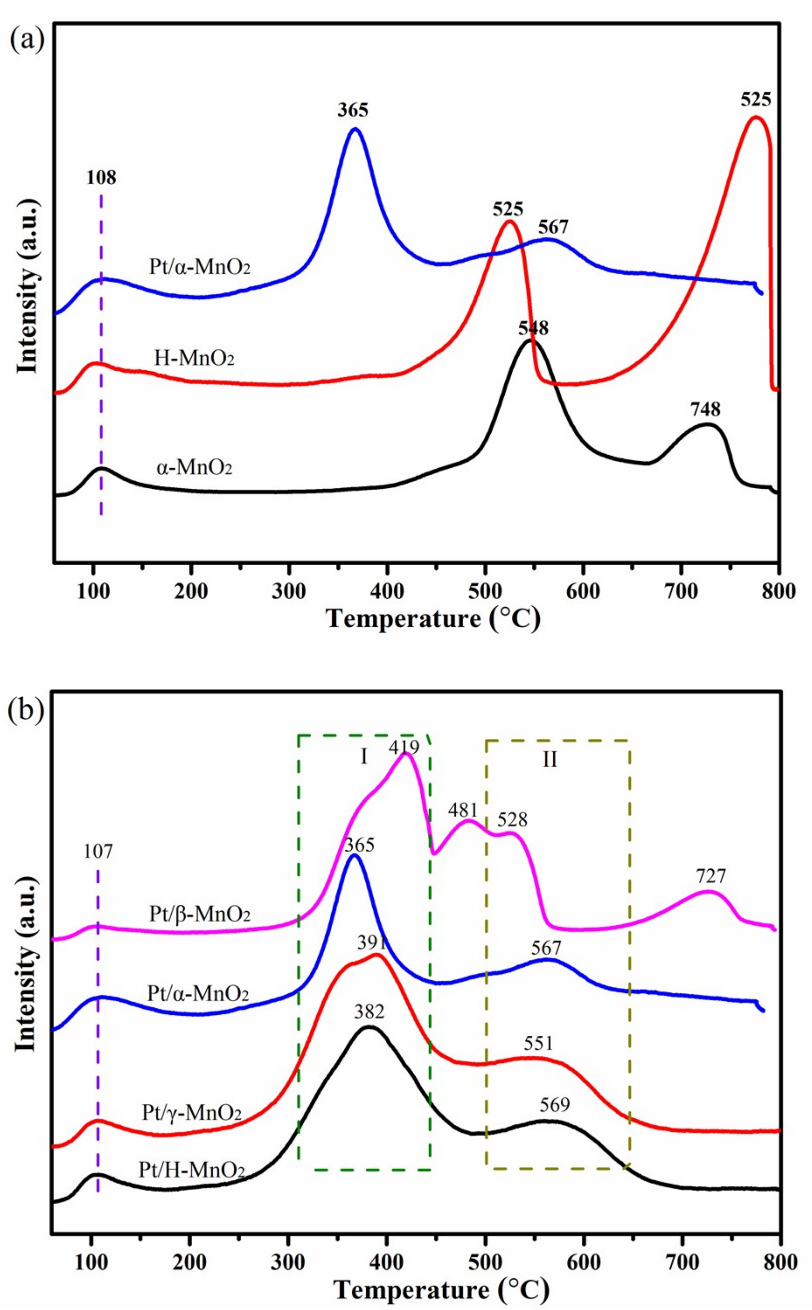

Fig. S7 O_2-TPD profiles of different MnO_2 and Pt/MnO_2 samples.

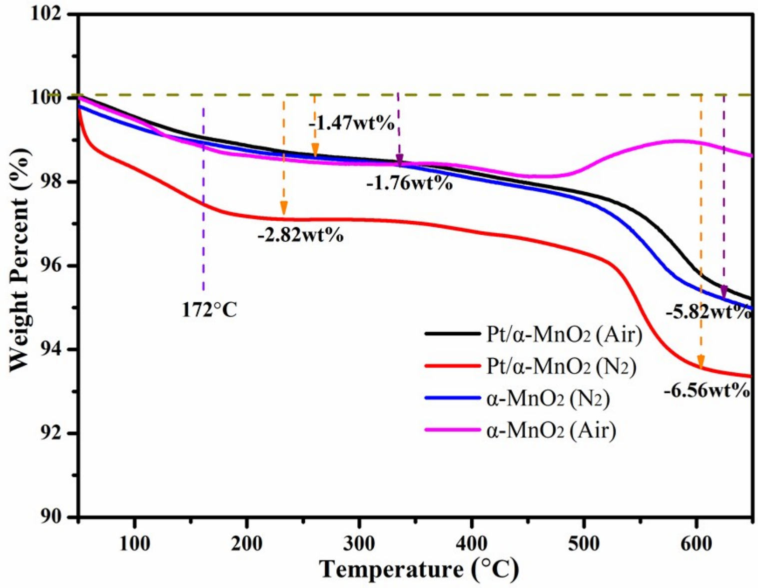

Fig. S8 thermogravimetric analysis of α-MnO_2 and Pt/α-MnO_2 samples at different atmospheres.

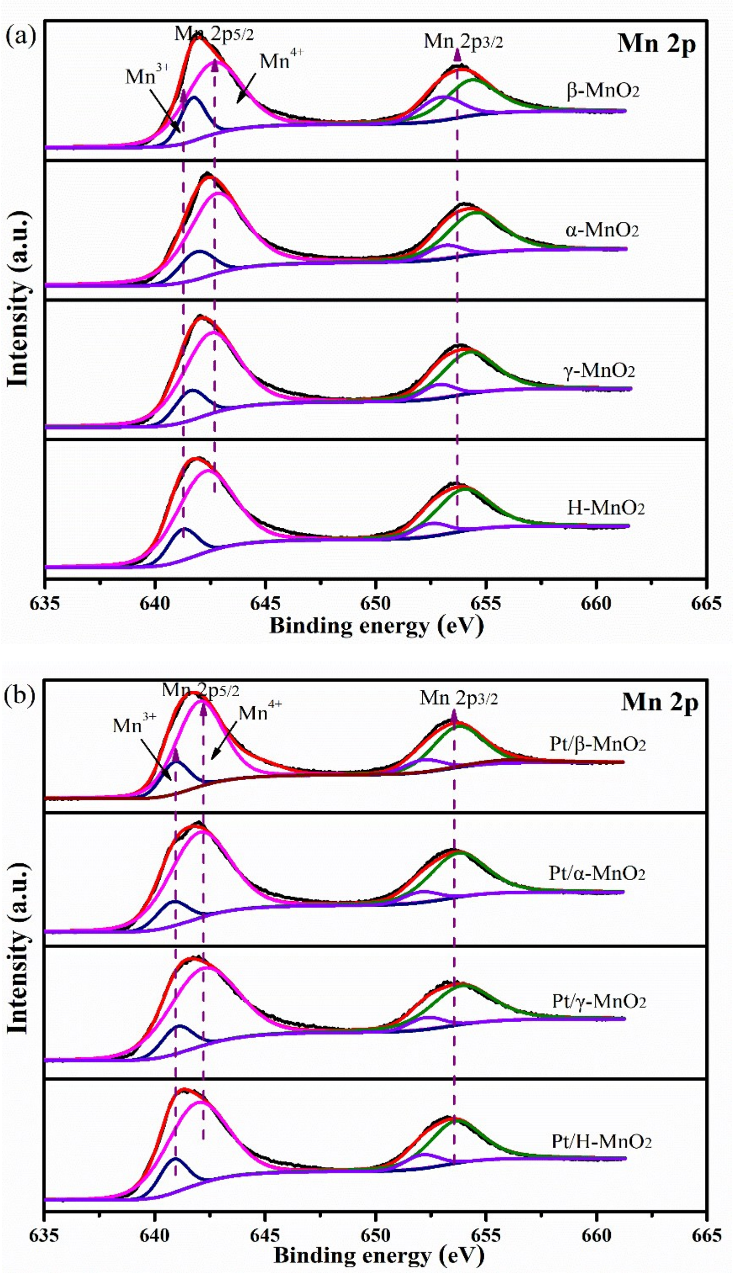
(a)
Mn 2p
Mn 2p5/2
Mn 2p3/2
Mn3+
Mn4+
β-MnO2
α-MnO2
γ-MnO2
H-MnO2
Intensity (a.u.)
635
640
645
650
655
660
665
Binding energy (eV)
(b)
Mn 2p
Mn 2p5/2
Mn 2p3/2
Mn3+
Mn4+
Pt/β-MnO2
Pt/α-MnO2
Pt/γ-MnO2
Pt/H-MnO2
Intensity (a.u.)
635
640
645
650
655
660
665
Binding energy (eV)

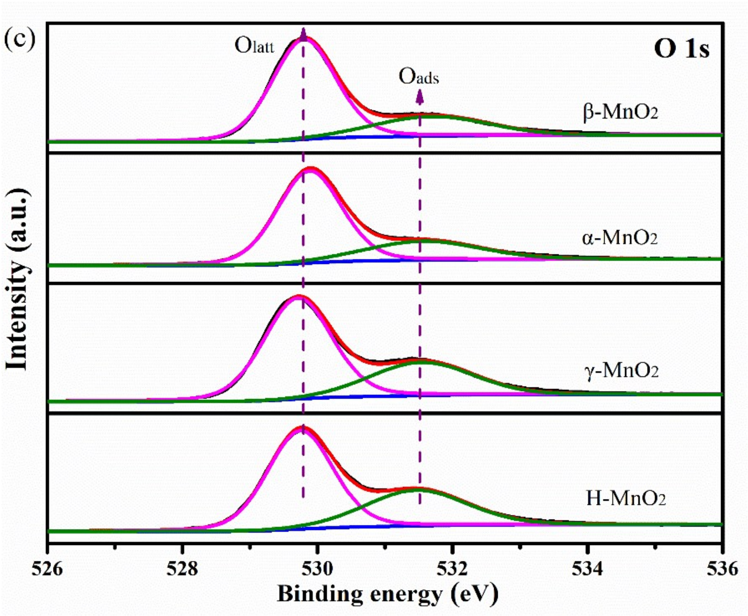

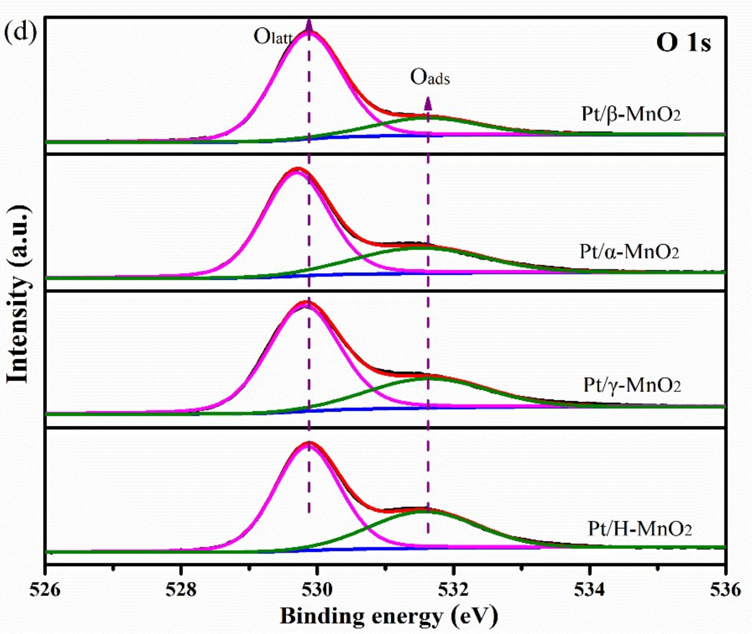

Fig. S9 (a, b) Mn 2p and (c, d) O 1s XPS spectra of different MnO_2 and Pt/MnO_2 samples.

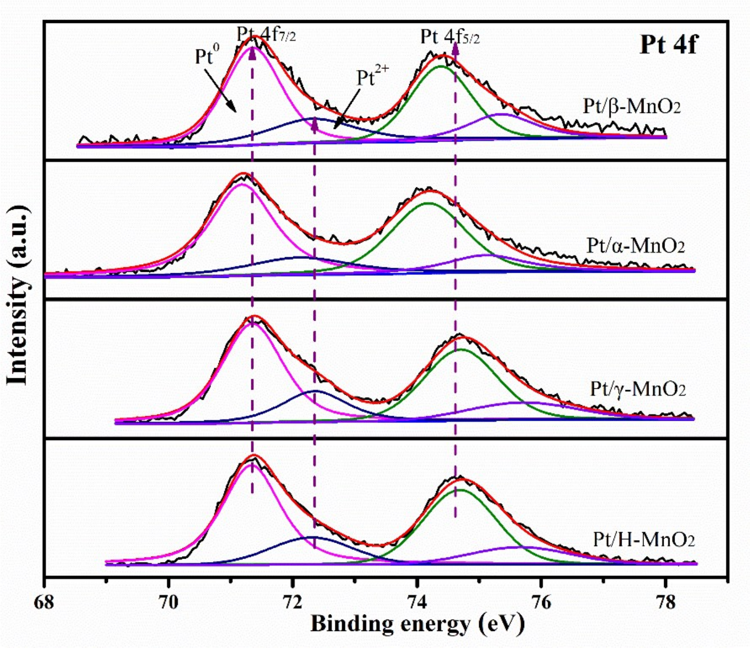

Fig. S10 Pt 4f XPS spectra of different Pt/MnO$_2$ samples.

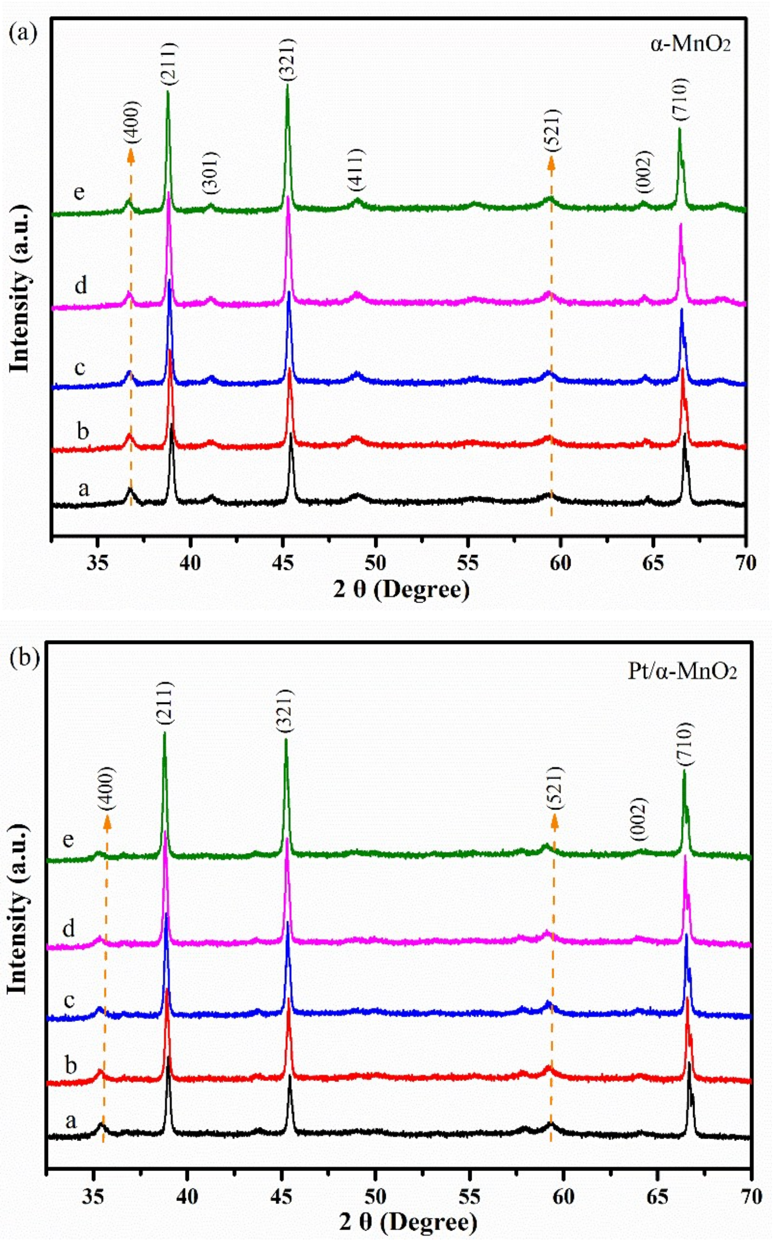

Fig. S11 HT-XRD patterns of (a) α-MnO_2 and (b) Pt/α-MnO_2 samples (Inserted labels a-e corresponding to 25, 100, 150, 200 and 250 ^{o}C, respectively).

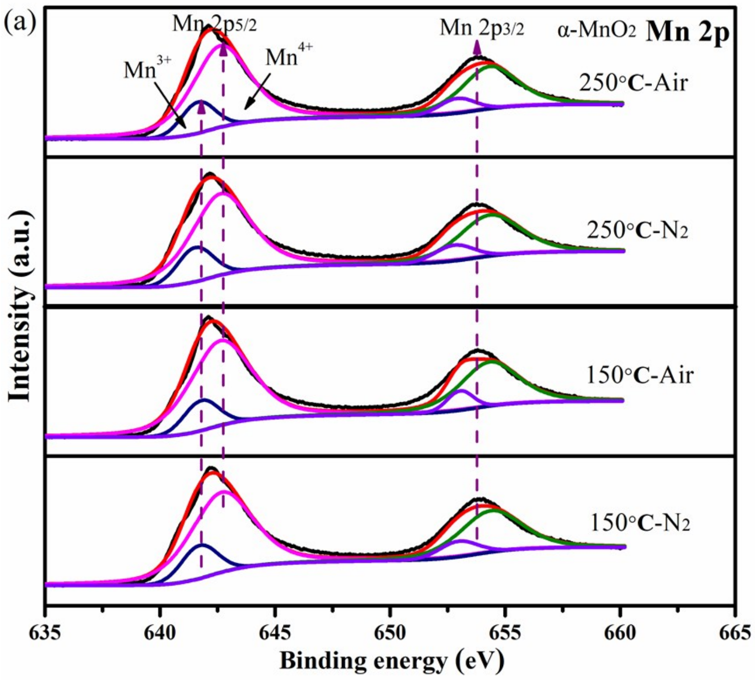
(a)
Mn 2p5/2
Mn 2p3/2
α-MnO2
Mn 2p
Mn3+
Mn4+
250°C-Air
250°C-N2
150°C-Air
150°C-N2
Intensity (a.u.)
635
640
645
650
655
660
665
Binding energy (eV)

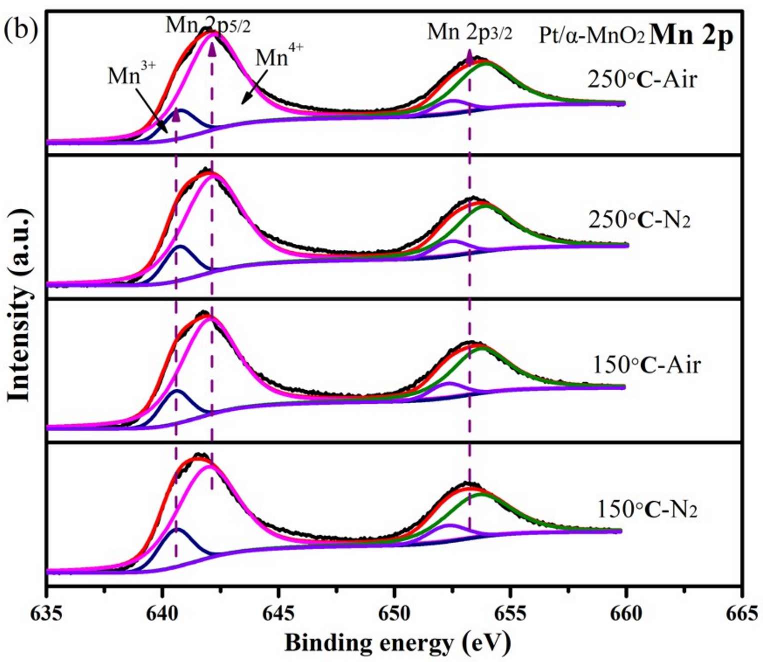
(b)
Mn 2p5/2
Mn 2p3/2
Pt/α-MnO2
Mn 2p
Mn3+
Mn4+
250°C-Air
250°C-N2
150°C-Air
150°C-N2
Intensity (a.u.)
635
640
645
650
655
660
665
Binding energy (eV)

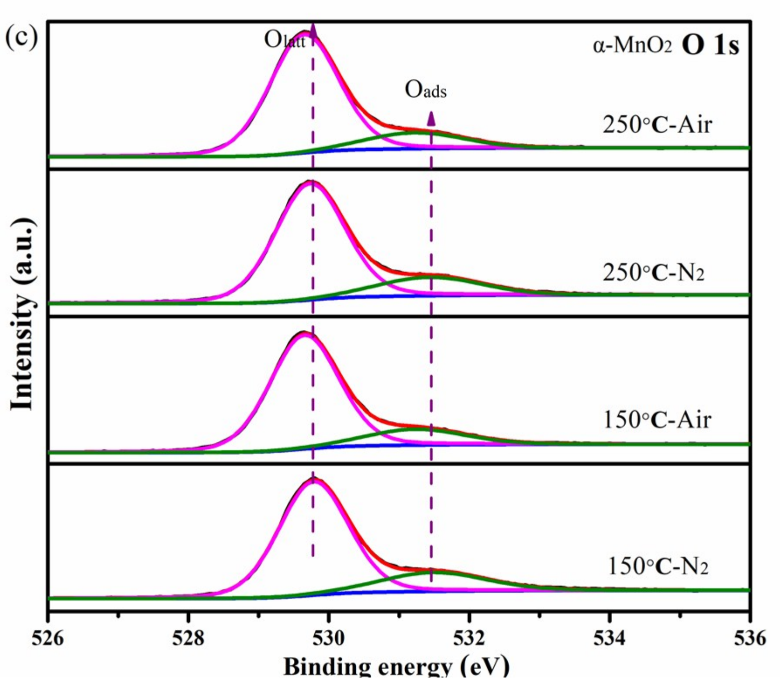

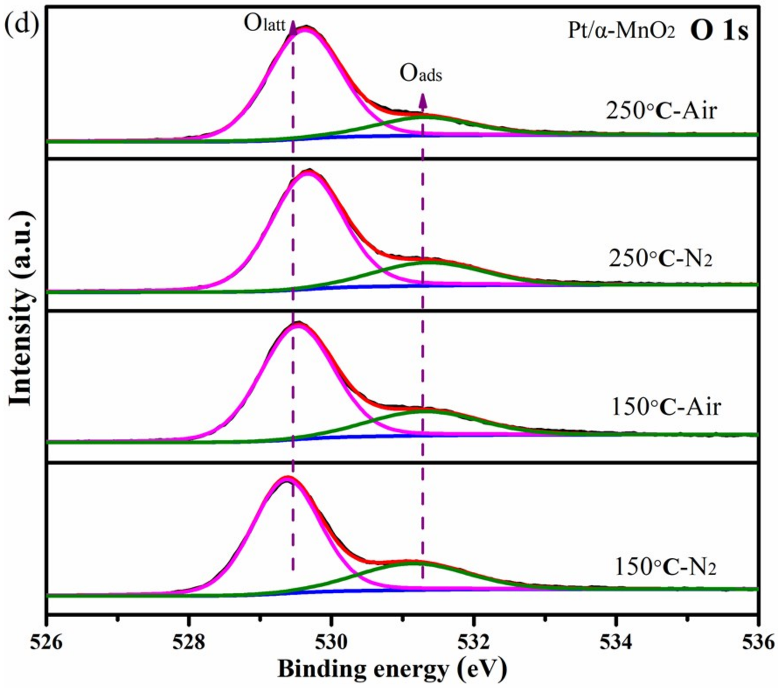

Fig. S12 (a, b) Mn 2p and (c, d) O 1s XPS spectra of α-MnO_2 and Pt/α-MnO_2 samples at different temperatures (150 and 250 °C) and atmosphere (N_2 and Air).

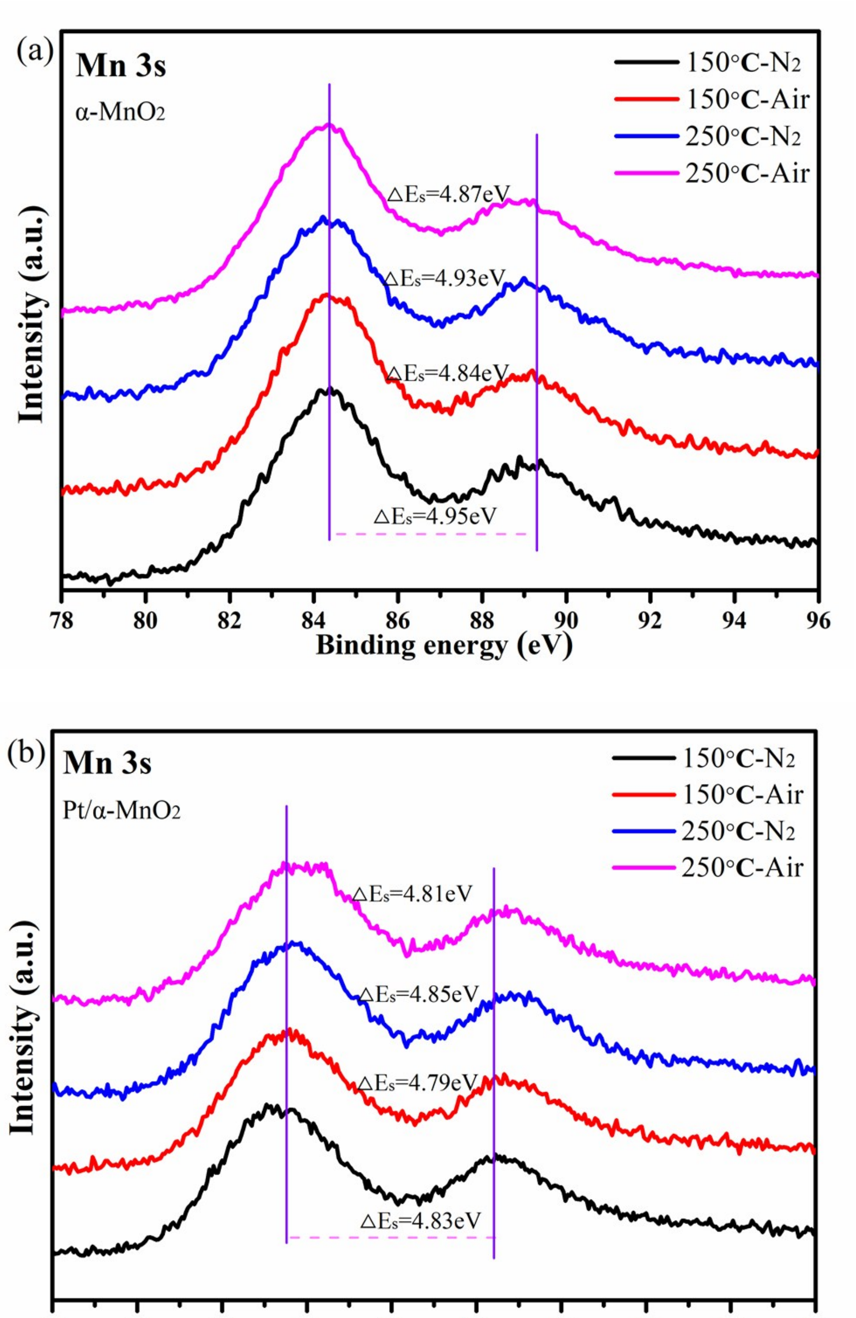

Fig. S13 Mn 3s XPS spectra of (a) α-MnO_2 and (b) Pt/α-MnO_2 samples at different temperatures (150 and 250 °C) and atmosphere (N_2 and Air).

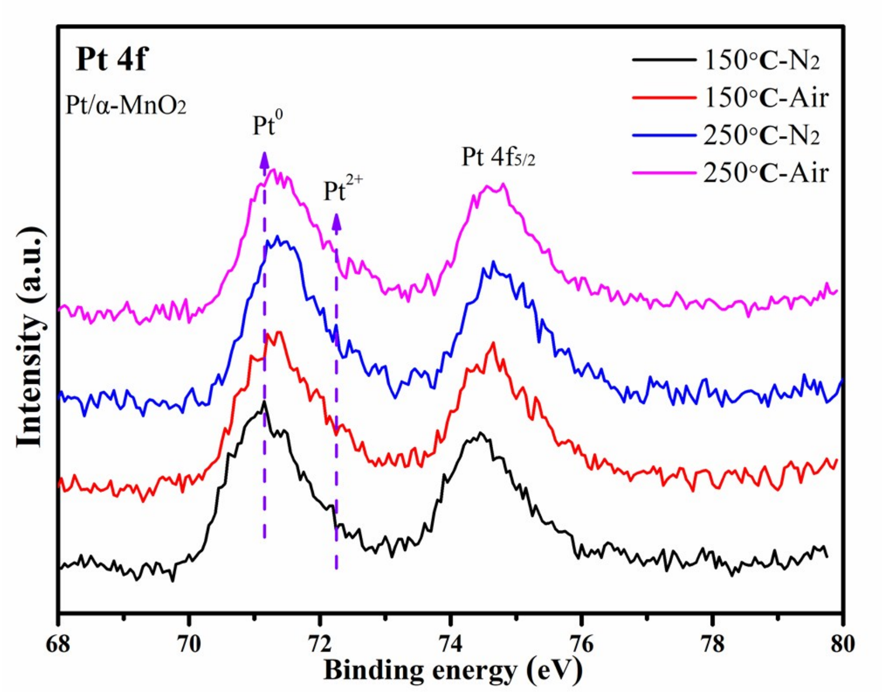

Fig. S14 Pt 4f XPS spectra of Pt/α-MnO$_2$ sample at different temperatures (150 and 250 °C) and atmosphere (N$_2$ and Air).

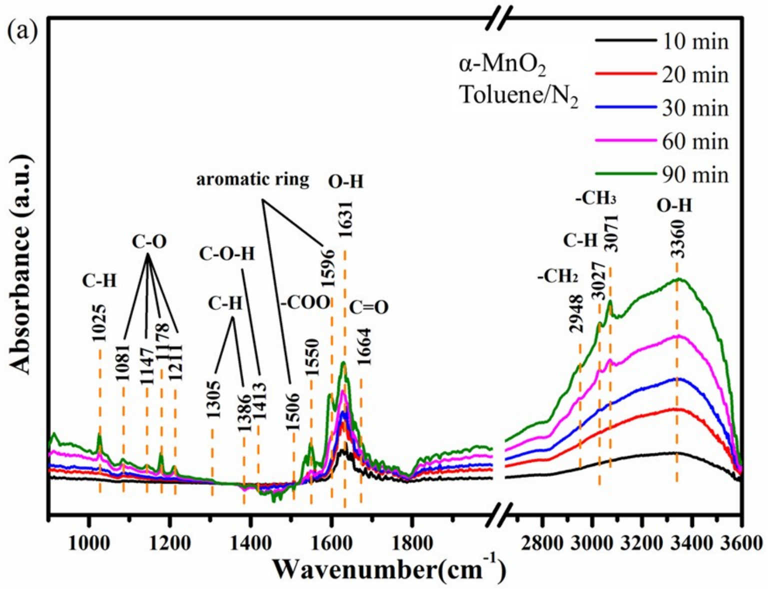
(a)
α-MnO$_2$
Toluene/N$_2$
10 min
20 min
30 min
60 min
90 min
Absorbance (a.u.)
C-H
1025
C-O
1081
1147
1178
1211
C-H
1305
1386
C-O-H
1413
aromatic ring
1506
-COO
1550
1596
O-H
1631
C=O
1664
-CH₂
2948
C-H
3027
-CH₃
3071
O-H
3360
1000
1200
1400
1600
1800
2800
3000
3200
3400
3600
Wavenumber(cm^{-1})

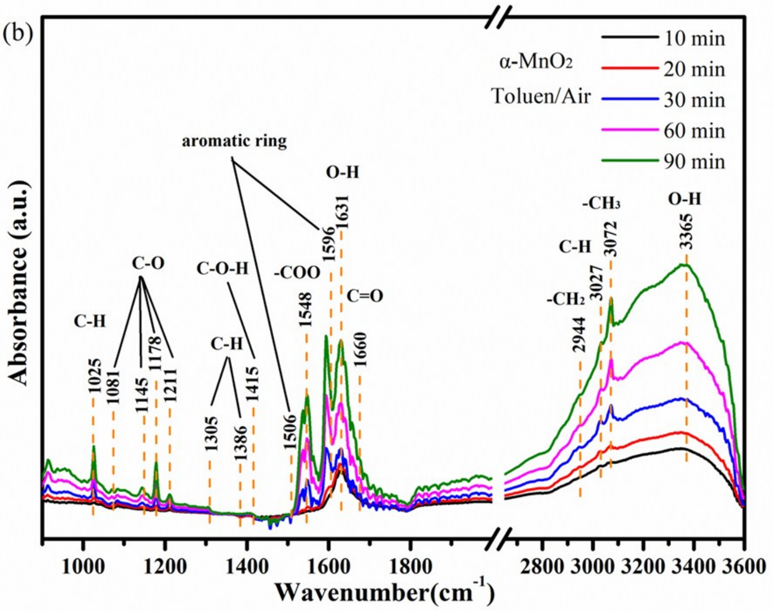
(b)
α-MnO₂
Toluen/Air
10 min
20 min
30 min
60 min
90 min
Absorbance (a.u.)
C-H
1025
C-O
1081
1145
1178
1211
C-H
1305
1386
C-O-H
1415
aromatic ring
1506
-COO
1548
1596
O-H
1631
C=O
1660
-CH₂
2944
C-H
3027
-CH₃
3072
O-H
3365
1000
1200
1400
1600
1800
2800
3000
3200
3400
3600
Wavenumber(cm^{-1})

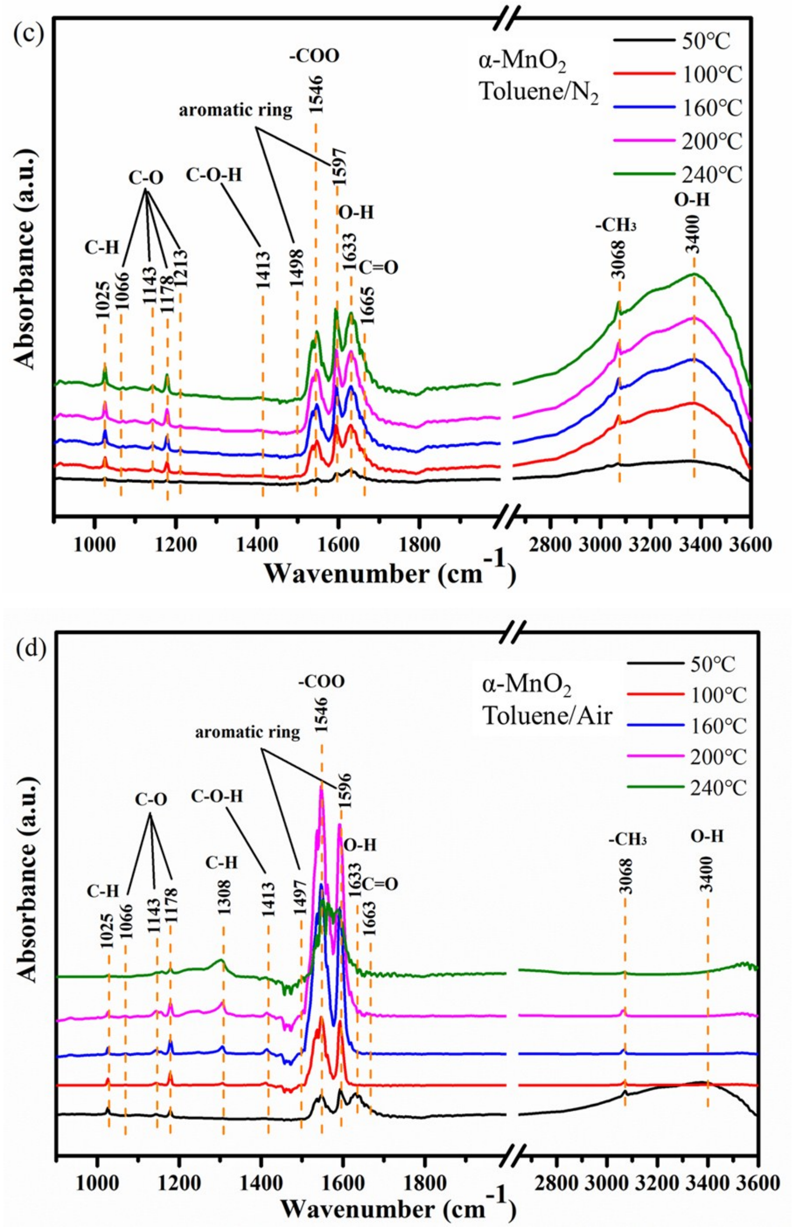

Fig. S15 In-situ DRIFT spectra of α-MnO_2 exposed to 500 ppm toluene/N_2 and toluene/Air at 50 °C for (a, b) different time, and at (c, d) different temperatures (50, 100, 160, 200 and 240 °C), respectively.

Table S1 the quasi in-situ XPS data for α-MnO_2 and (b) Pt/α-MnO_2 samples.

	α-MnO_2				Pt/α-MnO_2			
	150-N_2	150-Air	250-N_2	250-Air	150-N_2	150-Air	250-N_2	250-Air
Mn^{4+}/Mn^{3+}	5.14	6.02	4.93	5.55	6.71	7.34	6.63	7.01
O_{ads}/O_{total}	0.201	0.165	0.182	0.151	0.261	0.228	0.219	0.191
Mn 3s	4.95	4.84	4.93	4.87	4.83	4.79	4.85	4.81
AOS	3.36	3.48	3.38	3.45	3.49	3.54	3.47	3.51

AOS = 8.95- 1.13ΔE_s (eV)

MnO (Mn^{2+} ～ 6.0 eV)　Mn_2O_3 (Mn^{3+} ～ 5.3 eV)　MnO_2 (Mn^{4+} ～ 4.7 eV)